TRANSACTIONS OF THE INSTITUTE OF FLUID-FLOW MACHINERY

No. 133, 2016, 131–144

Tomasz Pałczyński*

Resonant characteristics of flow pulsation in pipes due to swept sine constraint

Institute of Turbomachinery, Lodz University of Technology, 219/223 Wólczańska, 90-924 Łódź, Poland

Abstract

A fast and easy to use method for analysing the amplitude frequency characteristics of pulsating flow in pipes with a sine sweep input function is presented. The key element is the sweeping excitation of the pulse generator frequency which generates fast whole-spectrum resonance (from 20 Hz to 160 Hz). A case study describes tests conducted into the applicability of the method for research into pulsating flows. First, the test rig is briefly described, along with the main assumptions of the research. Next, the amplitude frequency resonance due to swept oscillations is estimated for increasing, decreasing and changeable input mass flow rates. These characteristics are approximated based on a second-order transfer function. Following such assumptions, the damping coefficients and resonance frequencies are estimated. The influence of the direction of the frequency sweep method (increasing or decreasing) on the resultant resonance frequency is also investigated.

Keywords: Pulsating flow in pipes; Sweep sine excitation; Amplitude frequency characteristics

1 Introduction

The purpose of this work was to estimate the amplitude frequency characteristics of pulsating flows in pipes with a sine sweep input function. Sweep harmonic constraints enable faster acquisition of whole-spectrum resonance characteristics. The sweep input is a natural extension of the classical sinusoidal signal used for dynamic system response testing. This method is required for simulations

*Email address: tomasz.palczynski@p.lodz.pl

designed to estimate body characteristics. It is commonly used in turbomachinery (for spectral and modal analysis of rotors [1]), process and mechanical engineering (sine sweep vibration testing), acoustics [2,3] and automotive engineering (sweeping automotive suspension [4]). The proposed method was used in acoustic investigation of pipe flows [5]. Sweeping was limited to only one tone in each sweep step, because of the high level of turbulent noise generated by the mean flow [6]. Multireference sine sweep tests are conducted in the aircraft industry for estimating ground vibrations. Testing time can be minimized and the block size maximized by performing wrapped sweeps, in which the frequency difference between each source is maximized over the full frequency range of the test [7]. However, to the best knowledge of the author, no results have been published for swept inputs and pulsating flows in pipes. In particular, ions of investigations of the influence of down- and up-sweep input method on the resultant resonance frequency are presented.

The main contributions of this paper are the following:

- Real measurements taken during transitional states of pulsation frequency changes (from 40 Hz to 160 Hz) in pipes.
- A simplified Simulink model designed to estimate local pulsation amplitude and amplitude-frequency characteristics.
- An analysis of the influence of frequency change in a range of amplitudes from 40 Hz to 160 Hz on air pressure during pulsation change at three control sections.
- Measurements showing resonant frequency changes with increasing and decreasing pulsation frequencies.
- Proposed parameters for estimating second-order inertial elements (the damping coefficient and resonant frequency) to describe the observed phenomena.

1.1 Basic principles of the investigation

The laboratorytest rig was built to research the transitional states of changing pulsation frequencies in pipes. The main features of the test rig are presented in Fig. 1, including the pulse generator (PG) and three control sections (0, K, 3). The main flow parameters required to evaluate pressure, temperature and mass flow were measured at three control sections. The test procedure also examined the frequency change domain, in terms of initial and final conditions. The change in frequency was calculated based on the step function. Finally, the amplitude frequency characteristics were estimated using the curve fitting function in Matlab software [8]. This estimate was based on second-order inertial elements, and provided quite a good representation of the acquired data.

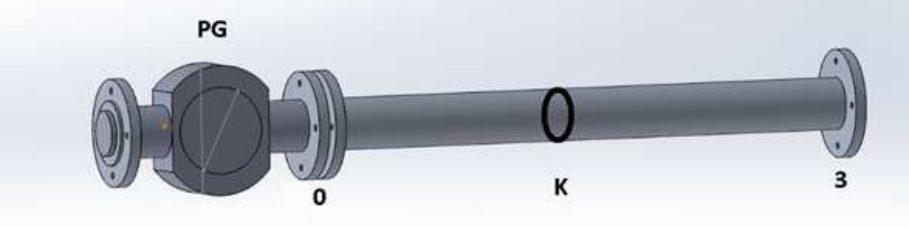

Figure 1: Main elements of the test rig with tested pipe [10]: PG – pulse generator, O, K, 3 – tested cross sections.

2 Measurement procedure

The proposed method for identifying swept amplitude-frequency characteristics can be summarized as follows, Fig. 2:

- The swept pulsation frequency change is set using an inverter connected to an electric motor. This system drives the pulse generator using the ramp frequency constraint mode.
- The transient states of the analysed phenomenon are measured.
- The results are processed using commercial Matlab-Simulink environment, including: filtering of noisy signals, estimation of instantaneous wave parameters (amplitude, mean value), and determination of amplitude-frequency characteristics. Finally, second order oscillating element approximation parameters such as resonance frequency and damping coefficient are estimated.

The proposed method of swept frequency response characteristics estimation (SFRCE) couples accurate transient measurement with the possibilities provided by block diagram environment for medeling and simulation software. It is thereby possible for these characteristics to be processed and plotted automatically in a very short time after the measurements (about 2 min).

2.1 Setting sweep-ramp pulsation frequency changes

The NI USB 6259 high speed multifunction data acquisition (DAQ) module was used as an inverter controller. The analog output from DAQ devices (board), which was a standard voltage signal in a range from 0 V to 10 V, was transferred into a standard current signal (4–20 mA) using the Aplisens ZSP-41 signal converter. In this way, the inverter was switched to external frequency input (current type). This facilitated setting the ramp change (20 Hz per second) for the required inverter frequency. The frequency variation in the time domain is presented in Fig. 3. The high repeatability of the lines, which is clearly visible, confirms that

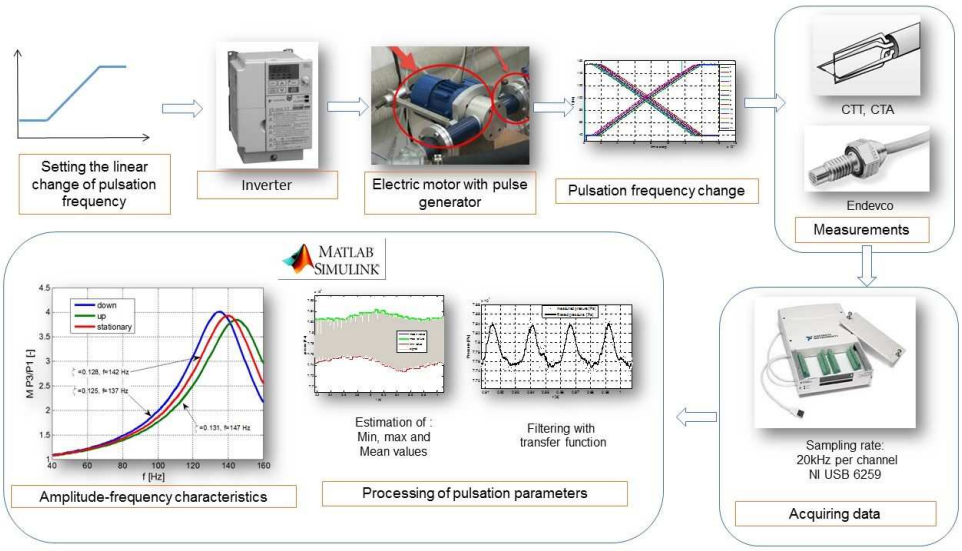

Figure 2: Method of estimating amplitude-frequency characteristics.

the average frequency change coefficient was equal to: $\triangle f/\triangle t = 20.09$ Hz/s, (see Tab. 1), (Δf – change of frequency, Δt – time step). The standard deviation of the achieved ramp coefficients was estimated as 0.043 Hz/s, based on the data in Tab. 1.

2.2 Measurement and acquisition of transient states

Figure 4 shows a test rig built at the Institute of Turbomachinery (Lodz University of Technology) for identifying amplitude-frequency characteristics in pipes with pulsating flow, following the procedure described above. Extensive research on dynamic phenomena in straight pipes supplied with a pulsating flow of gas shows that the variation of flow parameters (pressure, temperature, and velocity) depends on the nature of the pipe outlet [8,9,10]. Based on research by Olczyk [8], experimental data were incorporated into a simulation model, presented in [8,10]. The simulation and experimental parameters of the dynamic states of pulsating flow were compared. The results of their synthesis are presented below. The main parameters of the simulated flow were as follows [8]:

- range of desired values for the frequency of the pulse generator $f = 40$–160 Hz;
- pipe diameter $D_p = 42\ 10^{-3}$ m;

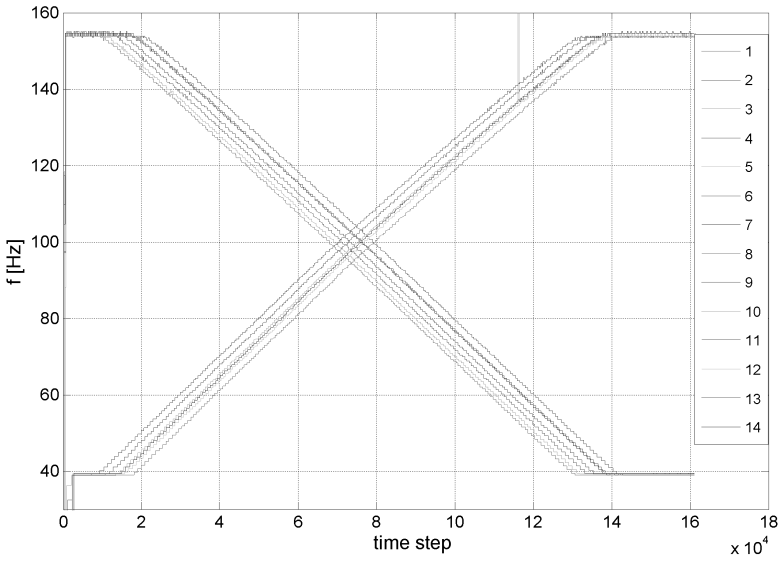

Table 1: Frequency change coefficient

series	$\Delta f/\Delta t$
1	20,15
2	20,02
3	20,13
4	20,08
5	20,07
6	20,11
7	20,14
8	20,02
9	20,10
10	20,09
11	20,06
12	20,05
aver.	20,09
std.dev.	0,043

Figure 3: Frequency variation in time step domain for fourteen test probes.

- pipe length $L_p = 0.544$ m, determined with resonance at 70 Hz and 140 Hz;
- nozzle diameter $D_n = 10 \times 10^{-3}$ m. The nozzle is mounted at one end of the pipe, at cross-section (3);
- desired flow temperature $T = 313.15$ K;
- mean flow speed $u = 20$ m/s (mean value);
- mean pressure $p = 115000$ Pa.

Transient and mean values for pressure, temperature and specific mass flow rate were measured at control sections (0) and (3), shown in Fig. 4. Transient pressure was also measured in section (K), located in the middle of the length of pipe (Fig. 1).

The pulse generator enables measurements of variable reliable and repeatable flow pulsations (Fig. 5). The stream line shown in the figure was prepared using Flow Express Package at Solidworks software [9]. This unit is almost frictionless and is driven by an electric motor with a variable speed drive (inverter) to control the speed of pulse generator rotor. The following equipment was used for measurements [8]:

- piezoresistive transducers for pressure measurements: Endevco 8510C-15 and 8510C-50 [10];

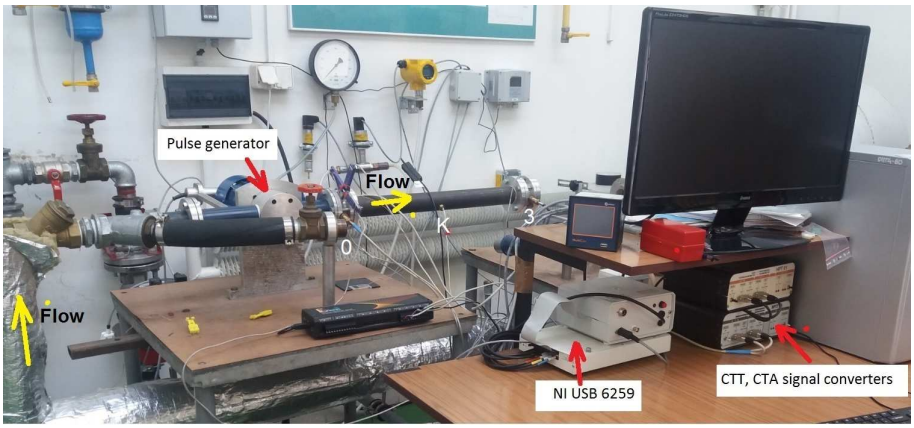

Figure 4: Test rig – general view.

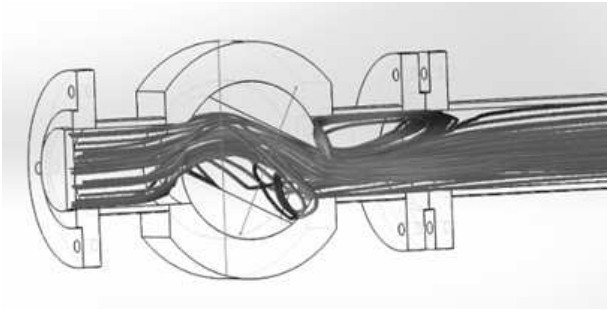

Figure 5: Flow visualization at pulse generator [8].

- constant current thermometers (CCT) for temperature measurements;
- constant temperature anemometers (CTA) for specific mass flow rate measurements.

The CCT and CTA probes used 5 lm tungsten wire.

2.3 Proces modeling and simulation

The Simulink model performs the following tasks:

- **Importing acquired transient flow parameters**. Signals from the test rig are imported into the workspace as an eight column array. The time domain for all compared series is the same: 20 kHz sampling frequency per channel and 160 000 probes, with an 8 s probe length for each series. The cyan blocks in Fig. 6 import the appropriate columns from the measured

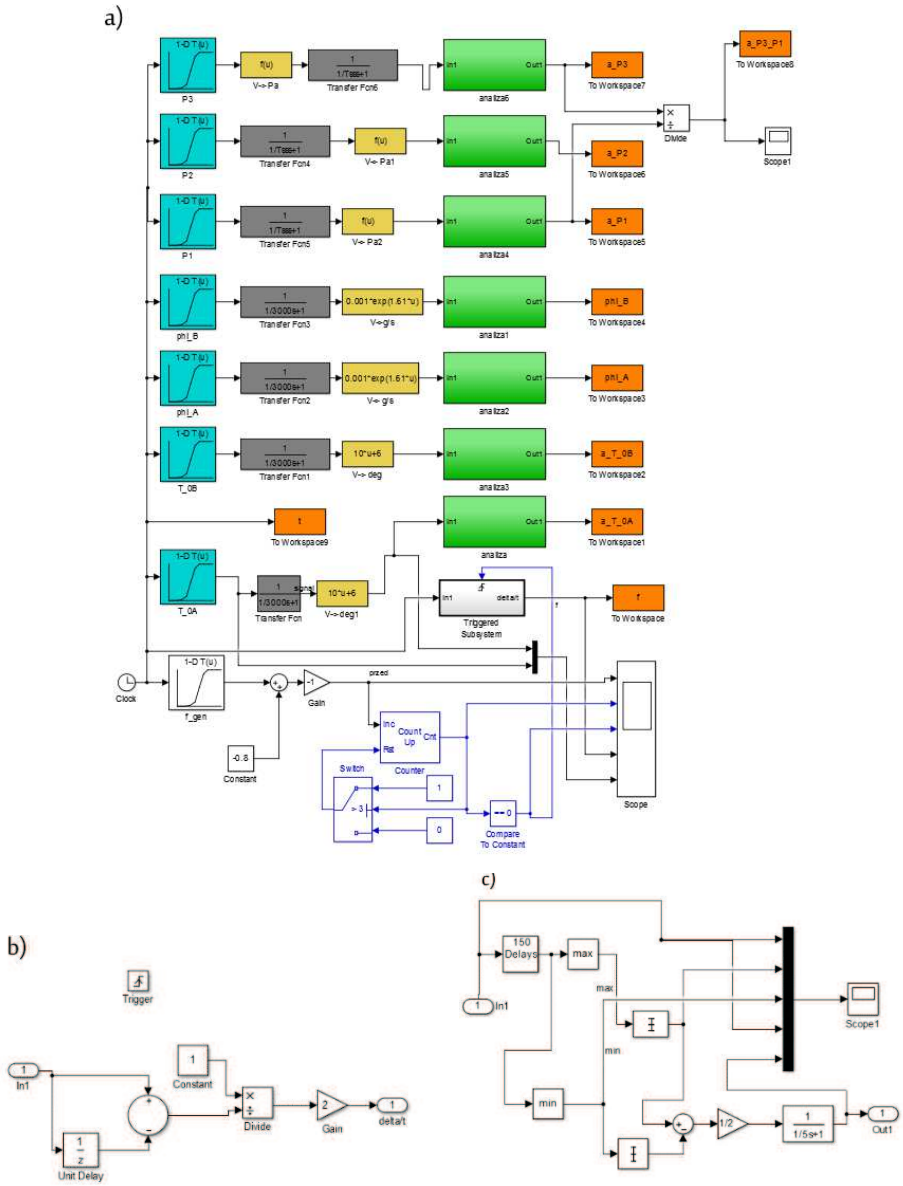

Figure 6: Simulink model of measurement data processing: a) frequency estimation, b) triggered subsystem, c) amplitude estimation.

array to generate transient signals in the simulation.

- **Filtering of noisy signals**. Because of the constant frequency changes produced by the pulse generator, a method of filtering noisy signals is used based on transfer function filtering (TFF). Classical fast Fourier transform (FFT) method cannot be applied in this case, because of the swept sine constraint (changing pulse generator frequency), where the base frequency should approximately constant. There are other commonly-used short windowing methods based on short time Fourier transform (STFT) [4], which, unlike wavelet analysis, do not limit precision in the time domain or the frequency range. The noisy signal is transmitted via the transfer function (which can be defined as a frequency function with a time constant of 1/3000 s), in dots in Fig. 6. The time constant is estimated by comparing the measured data with their filtered approximations, as shown in Fig. 7, to find a compromise between representative approximated values and their noisiness. The accuracy of the approximation is compared with nonswept measurements and with a standard FFT approximation (with eight harmonics), resulting in a correlation coefficient of about 0.98. The noisy range is estimated with the first-order derivate of the corresponding filtered parameter.

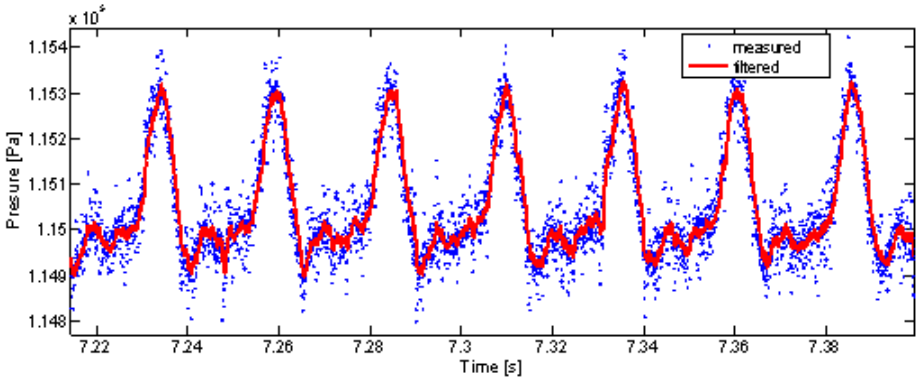

Figure 7: Comparison of measured data with their filtered approximations.

- **Measured signal processing**. Transfer of measured signals (0–10 V, 0–250 mV) is performed using the static characteristics of the appropriate transducers. Static characteristics are defined according to the calibration process described in detail in [15]. They are implemented into Simulink model as a user-defined function (in 'fen' simulink block);
- **Identification of time stamp**. A photoelectric revolution transducer gives

one peak per each revolution of the electronic-motor-drives. These peaks are also acquired for each measurement series. Counting the measured pulse generator frequency proceeds according to the following steps: counting the particular pulse and its transformation into a true/false signal ('counter' element of the model presented in Fig. 6a); 'Counter' element of triggered measurement of the time between two peaks (indicates time of the one particular pulse generator revolution) and then the frequency is estimated (model presented in Fig. 6b).

- **Identifying the amplitude of the pulse transient parameter.** Transient parameters (temperature, mass flow rate and pressure) are estimated by finding their maxima and minima, then their averages calculated, and finally the amplitude of the pulse is estimated, as presented in Fig. 6c. Data processed in this manner are shown in Fig. 8.

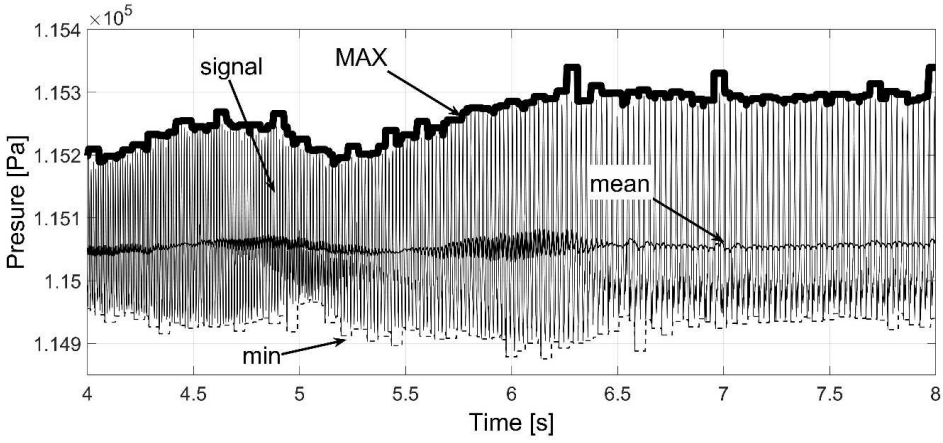

Figure 8: Graphical representation of amplitude estimation algorithm.

- **Amplitude-frequency characteristics.** Having estimated the amplitude of the analysed parameters, it is possible to calculate the quotient of amplitudes at two crucial cross-sections (0) and (3), $P3/P0$, for pressure amplitude-frequency characteristics (Fig. 9). Approximation is made using Eq. (1) [4] and the Curve Fitting Tool, using custom equation settings and default 95% confidence bounds.

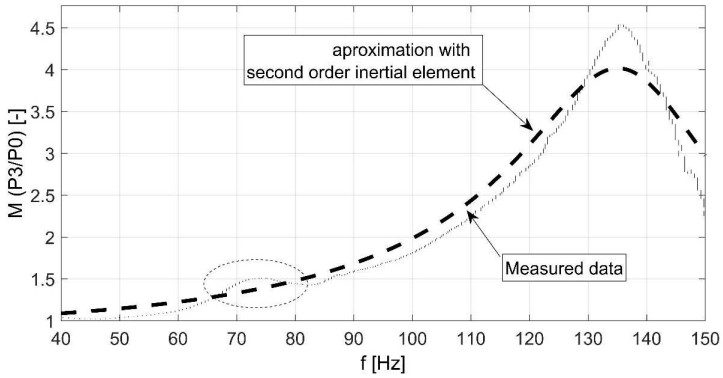

Figure 9: Amplitude-frequency characteristics of pressure in two cross-sections ($P0$ and $P3$).

$$M(f) = \left\{ \left[1 - \left(\frac{f}{f_n} \right)^2 \right]^2 + \left[\frac{2\zeta f}{f_n} \right]^2 \right\}^{-1/2}, \tag{1}$$

where: $M(f)$ – magnitude of oscillations, f – frequency, f_n – resonance frequency, ζ – relative damping coefficient.

3 Experimental results

The results of the research program presented in Fig. 10 and Tab. 2 are as follows:

- Increasing (147 Hz) and decreasing (137 Hz) the rotary speed of the pulse generator results in different resonant frequencies. These are caused by the acoustic phenomenon in the tested object, which results in hysteresis of the proposed approximation with second-order oscillating elements.
- The amplitude-frequency characteristics has been estimated using second-order inertial elements. The damping coefficient was 0.125 when the rotary speed was decreased and 0.131 when it was increased (see Fig. 10).
- The resonant frequency for the stationary case as a mean value of the two previously mentioned probes has been found (see Fig. 10). Parameters calculated in this way are comparable with stationary results reported in [10].
- The influence of the mass flow rate on the damping coefficient, approximated using the second-order oscillating transfer function, has been found. Because of the limited range of probes, it is difficult to determine the correlation function between the mean mass flow rate in pipes and the relevant damping

coefficient. Generally, increasing the mean mass flow rate decreased the damping coefficient in the proposed approximation of pulsating flows in the analysed pipe.

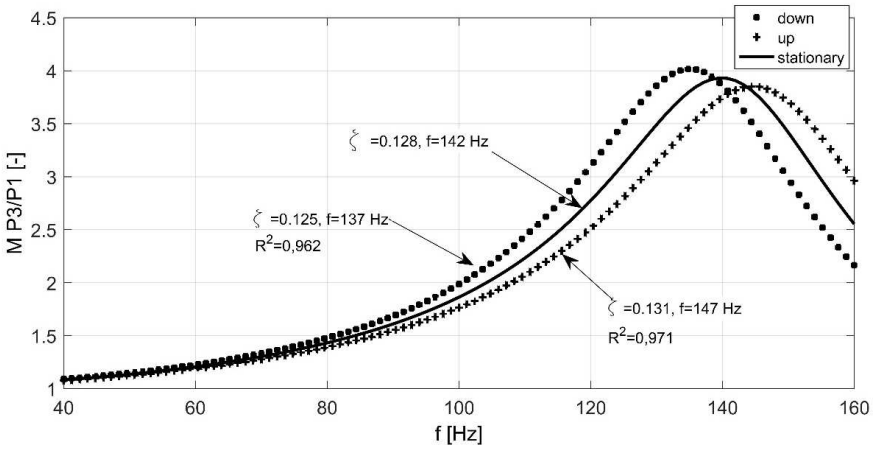

Figure 10: Amplitude frequency characteristics of pressure at two cross sections ($P0$ and $P3$) with increasing (up) and decreasing (down) pulsation frequency; ; ζ – relative damping coefficient [–], R^2 – coefficient of determination [–].

The tabulated results are given in Tab. 2. There are assumed the whole probes according to the presented method. There were procced presented procedures for each probe of the eighteens listed at the Tab. 2. The experiment covers three cases according to the mass flow rate domain (average rates 11, 22, 32×10^{-3} kg/s). For each case there were performed three sweeping up and three sweeping down probes. For all probes there were estimated magnitude of oscillations and relative damping coefficient.

4 Conclusion

The proposed method of swept frequency response characteristics estimation (SFRCE) couples accurate transient measurement with the possibilities provided by block diagram environment for modeling and simulation, employing a transfer function filtering method proposed by the author. Using this method, it was possible for swept frequency response characteristics to be processed and plotted automatically in a very short time once the measurements have been taken. It is also possible to create a 3D map showing the amplitude frequency characteristics for pressure in the tested pipe as a function of pulsation frequency and the

Table 2: Test series assumption.

No. of series	File name	Trend	Mass flow rate $\times 10^{-3}$ [kg/s]	Average mass flow rate $\times 10^{-3}$ [kg/s]	Magnitude of oscillations, $M(f)$ [–]	Average $M(f_n)$ [–]	Relative damping coefficient ζ [–]	Average relative damping coefficient
1	49	up	10.9	11	2.35	2.4	0.280	0.27
2	50	down			2.42		0.230	
3	51	up	11.1		2.36		0.290	
4	52	down			2.43		0.250	
5	53	up	11		2.31		0.300	
6	54	down			2.41		0.260	
7	55	up	22	22	3.5	3.6	0.220	0.21
8	56	down			3.8		0.198	
9	57	up	22.4		3.52		0.219	
10	58	down			3.76		0.200	
11	59	up	22.4		3.48		0.221	
12	60	down			3.83		0.196	
13	61	up	33	32	3.8	4.0	0.131	0.13
14	62	down			4.2		0.125	
15	63	up	32		3.75		0.128	
16	64	down			4.1		0.124	
17	65	up	31.9		3.82		0.130	
18	66	down			4.22		0.126	

mass flow rate function (Fig. 11). The main advantages of the method presented here are:

- acquisition of measurement data is ten times faster than measurements of each frequency separately;
- the inverter used in the test rig enables measurements for the sweep sine method because of the high stability of its 'amp' frequency excitation (see Tab. 1);
- an easy to use automatic algorithm for processing measurement data enables swept frequency response characteristics estimation just in a few minutes after measurements;
- it is also possible to indicate subharmonic frequencies, as shown in Fig. 9 in the dotted ellipse area. These subharmonics were not indicated in the approximation process because of the order level of the model (second order).

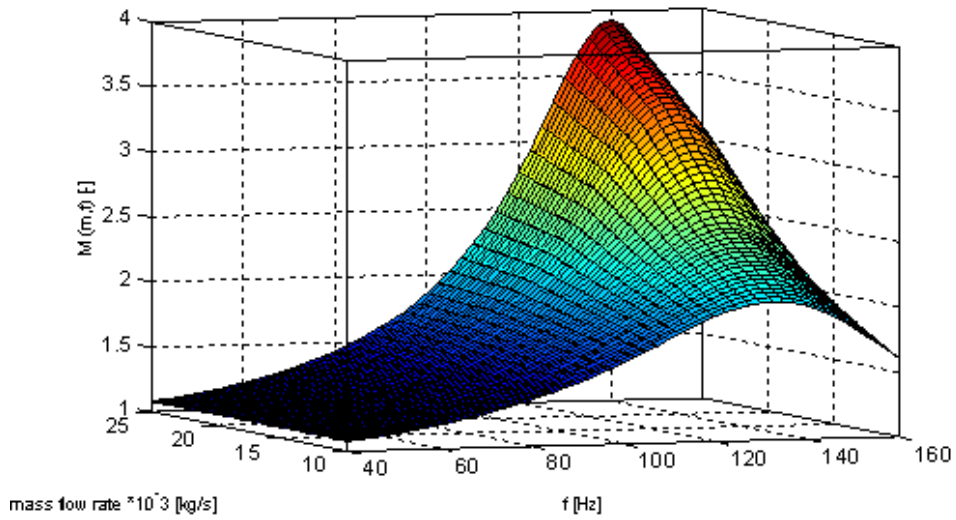

Figure 11: Amplitude frequency characteristics for pressure in tested pipe as a function of pulsation frequency and mass flow rate.

Received in July 2016

References

[1] Kozanecka D., Kozanecki Z., Łagodziński J.: *Active magnetic damper in a power transmission system.* Commun. Nonliner Sci. **16**(2011), 5, 2273–2278, http://dx.doi.org/10.1016/j.cnsns.2010.04.044.

[2] Farina A., *Simultaneous measurement of impulse response and distortion with a swept sine technique.* 108th AES Convention, Paris 2000.

[3] Müller S., Massarini P.: *Transfer-function measurement with sweeps.* J. Audio Eng. Soc. **49**(2001), 6, 443–471.

[4] Konieczny L.: *Analysis of simplification applied in vibrating damping modeling for passive car shock absorber.* Shock Vib. **2016**(2016), 6182847, http://dx.doi.org/10.1155/2016/6182847

[5] Kim Y.-., Kim S.H., Lim B.D. *et al.*: *Experimental study of acoustic characteristics of expansion chamber with mean flows.* KSME J. **2**(1988), 125, doi:10.1007/BF02953672.

[6] Price S., Smith D.: *Sources and remedies of high frequency piping vibration and noise.* In: Proc. 28th Turbomachinery Symp., http://www.engdyn.com/images/uploads/84-sources_and_remedies_of_high_frequency_piping_vib._and_noise-rev._-_drs&smp.pdf.

[7] Neapolitano K., Linehan D.: *Multiple sine sweep excitation for ground vibrations test*. In: Proc. IMAC-XXVII Feb. 9–12, 2009 Orlando, Florida, http://www.ata-e.com/uploads/2009_8.pdf.

[8] Olczyk A.: *Investigation of the specific mass flow rate distribution in pipes supplied with a pulsating flow*. Int. J. Heat Fluid Fl. **30**(2009), 4, 637–646, http://dx.doi.org/10.1016/j.ijheatfluidflow.2009.02.006, https://www.mathworks.com/help/curvefit/functionlist.html at 17.01.2017.

[9] Pałczyński T.: *A boundary conditions at modeling 1-D pulsating flows in pipes according to the method of characteristics*. KONES J. **19**(2012), 2, 395–402, http://www.solidworks.com/sw/products/simulation/floxpress.htm at 17.01.2017.

[10] Pałczyński T.: *1D model of pulsating flows in pipes dynamics using MOC*. In: Proc. 13th Int. Conf. Dynamical systems – theory and applications, Lodz 2015, https://www.endevco.com/8510c-15/ at 17.01.2017.